JOURNAL OF MATERIALS SCIENCE 33 (1998) 4569–4579

Observation of crack growth in PMMA with a low short glass fibre content by optical interferometry

M. KITAGAWA, A. KAI
Department of Human and Mechanical Systems Engineering, Kanazawa University, Kodatuno 2-40-20, Kanazawa, Japan

N. KOYAMA
Department of Energy Systems, Hachinohe Institute of Technology, Ohbiraki, Hachinohe, Japan
E-mail: masayosi@t.kanazawa-u.ac.jp

In order to investigate the effect of short glass fibre on crack growth, the crack tip was observed using double-cantilever beam samples machined from injection-moulded PMMA plates with a low short glass fibre content by means of optical interferometry. It was shown that the interference fringes were distorted around the fibre crossing the crack planes over a region two to four times larger than the fibre diameter, and that the fibre depressed the crack opening due to bridging between the crack planes, thus shortening the craze zone length in front of the crack tip and reducing the crack growth rate, leaving the arrest line on the fracture surface.

1. Introduction

Fracture mechanisms of short fibre-reinforced plastics have been investigated extensively [1]. In the regions where the fibres are perpendicular to the loading direction, failure begins to develop by fibre matrix debonding. On the other hand, in the case where the fibre orientation is parallel to the loading direction, fracture is caused by some mechanisms such as fibre matrix debonding, fibre pull-out, fibre fracture and craze initiation at the fibre ends. These mechanisms were deduced by observing the fracture surfaces and the zig-zag crack profiles at the side surfaces of the specimen using practical materials. But they can be directly observed by optical microscopy using transparent polymers with a very low short glass fibres content, which may not be suitable for practical use.

Microscopic aspects of the interaction between the crack and fibres are very interesting, in understanding the crack growth mechanism in fibre-reinforced plastics (FRP). In order to make direct observation of the crack tip, practical materials are not suitable because the inclusion of many fibres render them opaque. If the specimen is taken from a transparent polymer which have very few fibres with a weight fraction up to 0.2% at most, it may be possible to observe the deformation process around the fibres in the interior as well as on its surface. If an optical interference method is applied to such materials, the effect of the fibre on the crack tip opening behaviour is expected to be observed directly.

Optical interferometry is very useful for observing the crack tip behaviour in transparent polymers. Excellent work on this subject has been published by Döll and co-workers [2, 3]. Schirrer [4] applied optical interferometry to investigate the mechanism of toughness improvement in rubber-toughened polymer, and considered that the technique is basically inadequate for rubber-toughened polymers where the high toughness is due to multiple crazing. This prevented any clean interference pattern, and interference fringes could be obtained around the fibres near the crack tip. This may be attributed partly to the small probability of rubber particles lightly mixed in the matrix polymer encountering and crossing the crack. However, glass if fibres are mixed into the matrix polymer in place of the rubber particles, observations of the interference between the crack and the fibre may become possible.

In this work, in order to understand fundamentally the effect of the glass fibre on the crack growth in the composite material, the optical interference method was applied to poly(methyl methacrylate) (PMMA) with a very low short glass fibre content.

2. Experimental procedure

2.1. Specimens

The dimensions of the double-cantilever beam (DCB) specimen used in this experiment are shown in Fig. 1. The DCB specimens are usually used to observe crack behaviour in polymeric solids. The specimens were machined from injection-moulded plates of PMMA with a very low short glass fibre content (SGF = 0.1 and 0.2 wt %) so that they might be perpendicular to the moulding direction. Side grooves were cut in the specimen to ensure that the crack direction was straight. The crack grows in the narrow plane

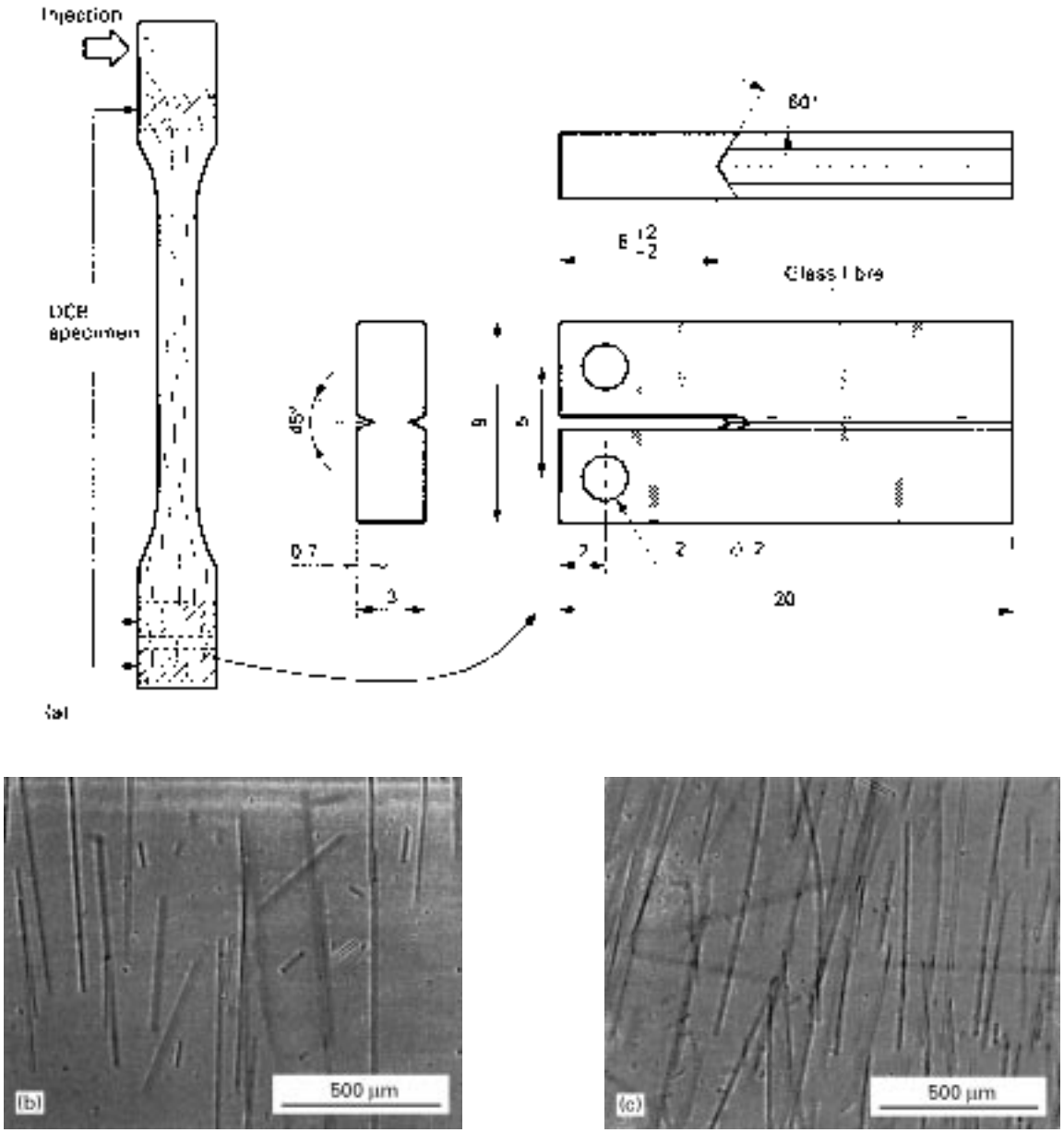

Figure 1 DCB specimen dimensions and materials. (a) DCB specimen machined from injection-moulded tensile specimen with rectangular cross-section 10 × 3 mm; (b, c) micrographs of short glass fibre PMMA composite with fibre weight fraction of 0.1 and 0.2 wt %, respectively.

indicated by the oblique lines in the top right-hand shown in Fig. 1a. The initial crack was introduced at a stress intensity factor range of 0.5 MPa $m^{1/2}$ at a frequency of 1–2 Hz by a home-made fatigue testing machine.

As may be expected from the mixed law for a composite material, the mechanical properties, such as elastic modulus, yield stress, fracture stress and fracture strain, are not very different from those of the matrix polymer, because of the low SGF content. The glass transition temperature of the PMMA was about 110 °C. The diameter of the silane-coated fibre was 11 μm, and the fibre length distribution was in the range 20–900 μm. The average values of fibre length and aspect ratio in the specimen were ~200 μm and 18, respectively [5, 6]. In such specimens, the crack is expected to cross a considerable number of the fibres placed in a perpendicular manner. If the matrix polymer is transparent, the deformation behaviour around the fibres inside the specimen can be easily observed through an optical microscope. Examples of specimens observed by a transmitted light optical microscope are shown in Fig. 1 where SGFs with different lengths are dispersed uniformly in the specimen. The details of the fibre length distribution are described elsewhere [5, 6].

2.2. Experimental apparatus

The apparatus used in this experiment is shown in Fig. 2. It is composed of a mini-fatigue testing machine, 1, an optical microscope for observing interference fringe patterns, 2, and an image processor, 3. The mini-testing machine, which is attached to the microscope, is controlled by a microcomputer, and is devised using a precision linear guide so that the lower loading pin can move along the vertical direction to allow the crack to grow in a straight line. The load is applied along the vertical direction of Fig. 1a, through the loading pins inserted into the pin holes of the

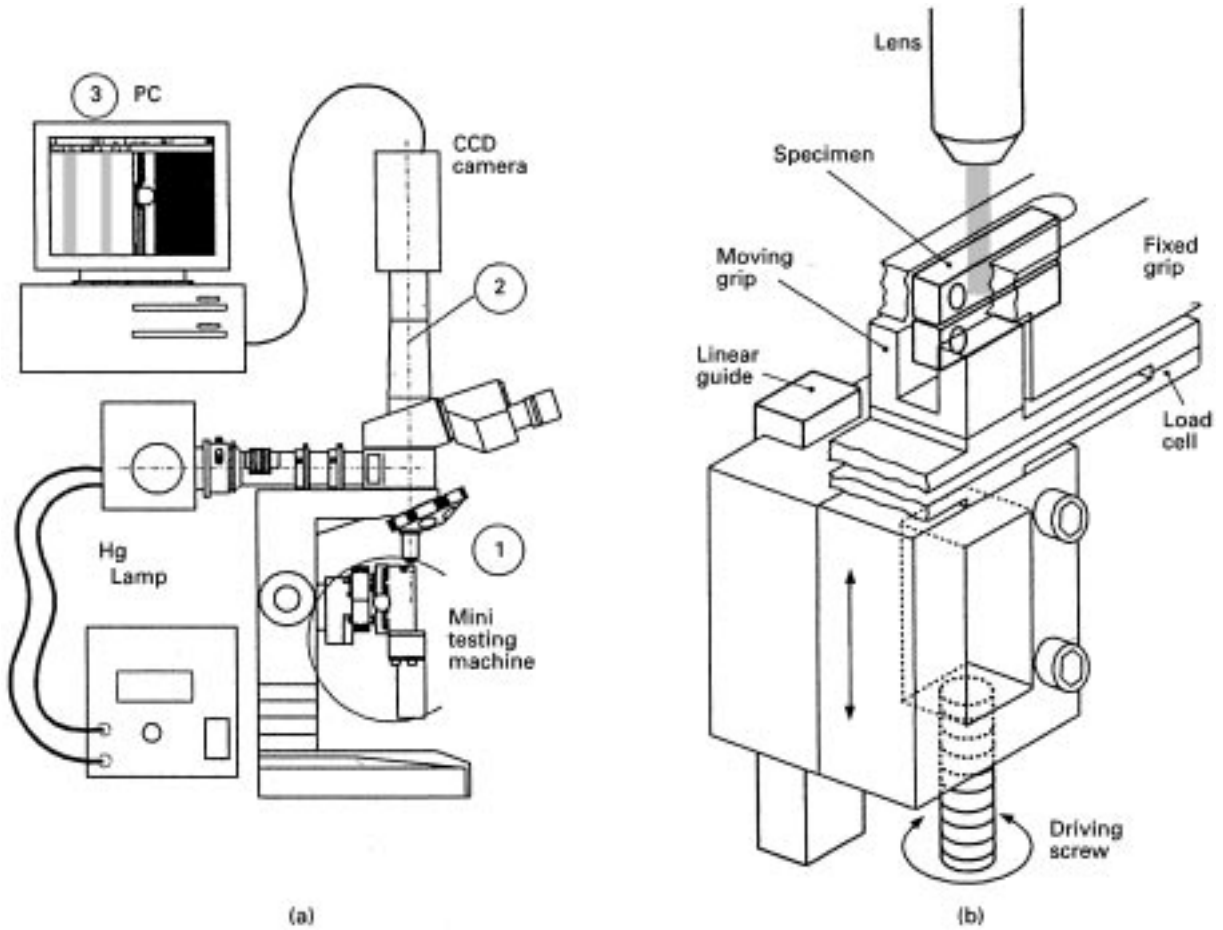

Figure 2 Schematic illustration of the mini-testing machine. (a) central view: 1, mini tensile testing machine; 2, optical microscope with mercury light source. 3, personal computer with image processor: (b) Enlarged view of the mini-testing machine.

specimen. The specimen is illuminated in reflection with a monochromatic mercury light of wavelength 546 nm under normal incident conditions.

The fringe patterns which arise from the interference between reflections from the crack planes were recorded using a video tape recorder through a CCD camera and were analysed by an image processor to describe the crack opening.

2.3. Experimental measurements

When the applied load increases and reaches a critical level (about 1 MPa $m^{1/2}$) for the crack to propagate, the distance between the specimen grips is held constant while the load gradually decreases with increasing time, due to both the visco-elastic effect and the increase in crack length; the crack ceases to grow at a stress intensity factor of about 0.7 MPa $m^{1/2}$. The time required for the start of the crack growth is about 200 s. During growth, the crack tip is observed through the microscope. The crack length (the distance from the pin hole to the crack front) varied from 6–11 mm during the test. After the crack growth test, the fracture surfaces corresponding to the interference fringe marks were observed through SEM. The crack growth tests were performed at room temperature $23 \pm 3\,^{\circ}C$.

An example of the fringe patterns obtained for a specimen which did not included SGF is shown in Fig. 3 where the fringe marks are not distorted. The crack growth direction is from left to right. The part where the fringe marks are dense denotes the craze region. The crack opening $2v(x)$ is calculated accurately by the luminosity distribution through a basic interference theory developed by Döll and co-workers [2, 3]

$$2v = n\lambda/2\mu \tag{1a}$$

or

$$(n - 1/2)\lambda/2\mu \tag{1b}$$

$$\mu = (1 + [0.6/(0.8 + \varepsilon)]^{1/2} \tag{1c}$$

$$n/n_0 = 1 + \varepsilon/1.32 \tag{1d}$$

where n and n_0 are the loaded and unloaded fringe orders at position x, respectively, ε is the strain, λ is the wavelength of the incident light and μ is the refractive index, $\mu_0 = 1.32$ is the unloaded refractive index of PMMA. For the calculation inside the crack, $\mu = 1$ is used. The calculated shape of the crack is plotted in Fig. 3. The curve based on the Dugdale model [7] approximated by Rice [8] is also shown

$$s = (\pi/8)(K/\delta_c)^2$$

$$2v(x) = (8\sigma_0 s)/(\pi E)\{\xi - (x/2s)\ln[(1 + \xi)/(1 - \xi)]\}$$

where E is the elastic modulus, σ_c is the craze stress which is assumed to be constant along the craze zone,

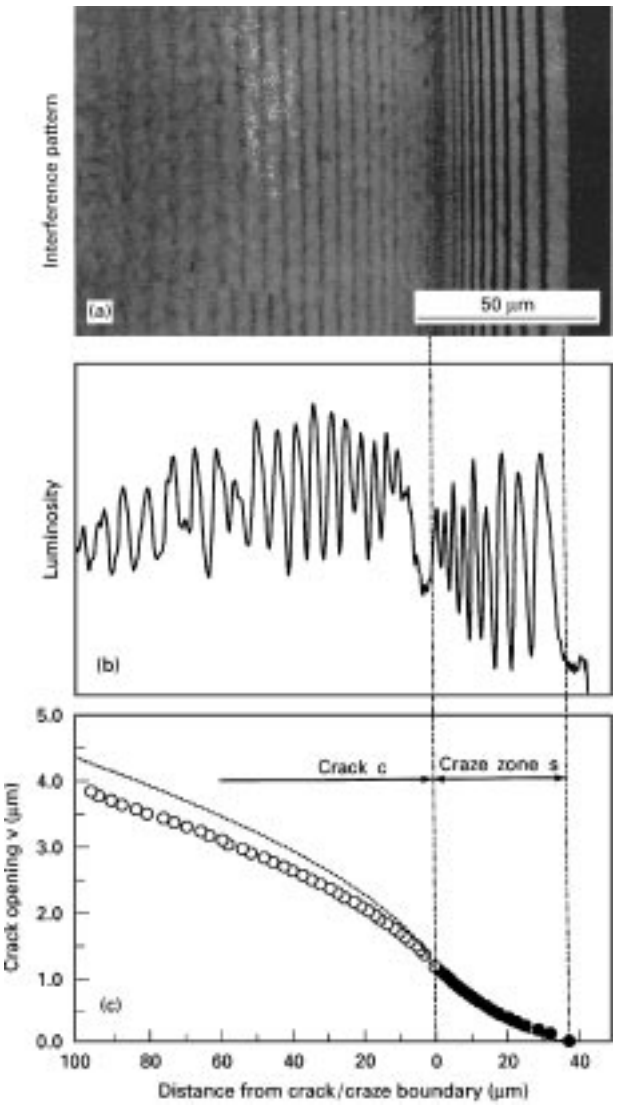

Figure 3 Example of (a) an interference fringe pattern (b) a luminosity trace obtained by an image processor, and (c) crack opening in PMMA without glass fibres (stress intensity factor = 0.7 MPa $m^{1/2}$). (○, ●) The shape of the crack, (- - - -) curve based on the Dugdale mode [7] approximated by Rice [8].

s is the craze length, K is the stress intensity factor, x is the length from the craze front, $\xi = (1 - x/s)^{1/2}$. The stress intensity factor K is calculated using the formula for the DCB specimen. The values of the craze stress and the elastic modulus used for the calculation are 70.3 and 2700 MPa, respectively. It was found that the crack opening shape, especially the cusp type in the craze zone, was described well by the simple Dugdale model.

3. Results and discussions

Fig. 4 shows the variation of the fringe patterns around the glass fibre near the crack tip with increasing crack length. First, the glass fibre encounters the craze tip in front of the crack (a), is completely surrounded by the craze region (b–d), reaches the craze/crack boundary (e, f), and finally enters the interior of the crack (g, h). The dark-shaded circles near the centre of the photographs denote the region which includes the glass fibres. The crack growth direction is from left to right. It is seen that the fringes around the glass fibre change their shape as the crack propagates from photographs (a) to (h).

Fig. 5 shows the variation of the crack length, craze zone length s, stress intensity factor, SIF, and the crack tip opening displacement CTOD, far from the fibre with increasing testing time. The A–A and B–B sections, respectively, we along the line passing through the glass fibre and along the line far from the fibre, as shown in Fig. 4. The values, except the craze zone length, are measured along section B–B. (a) to (h) in Fig. 5 correspond to Fig. 4a–h. The time is measured on the basis of the starting point of this test. The fracture surface corresponding to the change of the fringe marks is shown in Fig. 6, where the crack propagates from left to right.

When the craze zone in front of the crack tip encounters and crosses the fibre nearly perpendicular to the crack planes Fig. 4a and b, the craze tip becomes greatly distorted and its length is much smaller near to the fibre than in the region far away from the fibre. The fibre distorts the fringe patterns into a V-shape at the side of the craze tip (to the right of the fibre in the figure), while the fringe lines at the crack side (to the left of the fibre) are not so disturbed by the fibre, and are nearly straight and parallel to each other. As the crack grows and the fibre is completely surrounded by the craze region (c, d), the craze front again follows a straight line. The distorted area covers a distance two to four times larger than the fibre diameter. This distance may indicate a limit over which the single fibre can produce an effect on the crack opening. Until the fibre reaches the craze/crack boundary, the craze zone length at section A–A increases slightly, while its length at section B–B remains nearly constant. Between (f) and (g), the crack gradually reduced its speed, and near to stage (g), finally, the crack ceased to grow. After this stage, the crack began to grow again and simultaneously, the craze zone length suddenly decreased (h). When the fibre was inside the crack after passing through the craze region (g and h), the distortion of the fringe marks within the craze zone disappeared and were nearly parallel to each other.

At stage (g), the crack, which had been propagating continuously, ceased to grow for a while, as shown in Fig. 5. After some time, the crack began to grow again, and the arrest band which plausibly traces the distorted shape of the fringe pattern developed in the vicinity of the fibre, as shown in Fig. 6. This arrest line, which was generated probably at the crack–craze boundary, may be caused by the existence of the fibre. This may suggest a strong bridging of the fibre over the crack planes.

During the period shown in Fig. 4, both the crack growth rate and SIF decreased slightly. The craze zone length, s at section A–A increased steeply just after the craze tip encountered the glass fibre. When the fibre was completely inside the craze zone, the increase rate of s became small, until the crack/craze boundary reached the fibre. The length s decreased suddenly when the crack/craze boundary crossed the fibre and at this time, the crack stopped growing for a while, as shown in the upper part of the figure. In

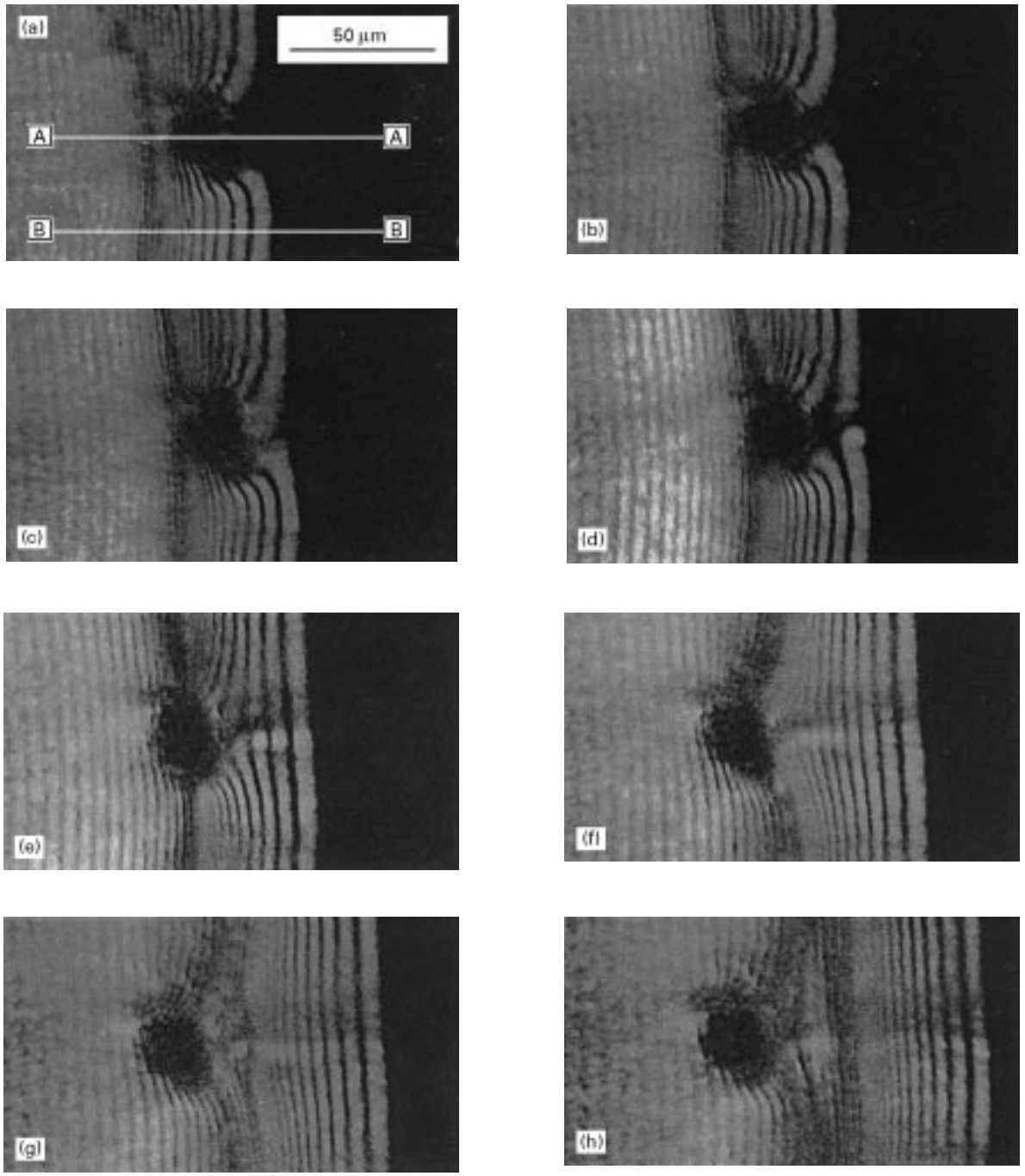

Figure 4 Variation of interference fringe patterns near the crack tip around a glass fibre perpendicular to the crack planes with crack growth in PMMA containing 0.2 wt % glass fibre. (a–h) correspond to Fig. 5a–h and Fig. 8a–h. Crack opening and craze length were measured in Fig. 5, along lines. A–A and B–B.

constant to such a big change of s at section A–A, the craze length at section B–B remained nearly constant during this period. The value of CTOD increased until the crack/craze interface was close to the fibre. At stage (g), the CTOD suddenly changed.

The fringe patterns observed when the crack grows around a single fibre perpendicular to the crack planes are schematically illustrated in Fig. 7 where the dark circular areas show the region including the fibre. When the fibre encounters the craze tip, the interference fringes are distorted in a V-shape over a region about four times longer than the fibre diameter in the vertical direction of the figure (the, direction parallel to the crack edge). When the fibre is completely within the craze region, the fringes are distorted over a distance of twice the fibre diameter only on the right hand side along the crack direction. The fringes on the left-hand side of the fibre are not distorted. The fringe about 20 μm away from the fibre becomes straight. These distances, which are four and two times longer in the directions vertical and horizontal, respectively, to the crack growth direction, may show a limit to the range influenced by the fibre bridging.

Fig. 8 shows the cracks morphology calculated from the fringe patterns corresponding to the photographs shown in Fig. 4. The solid curves denote the crack

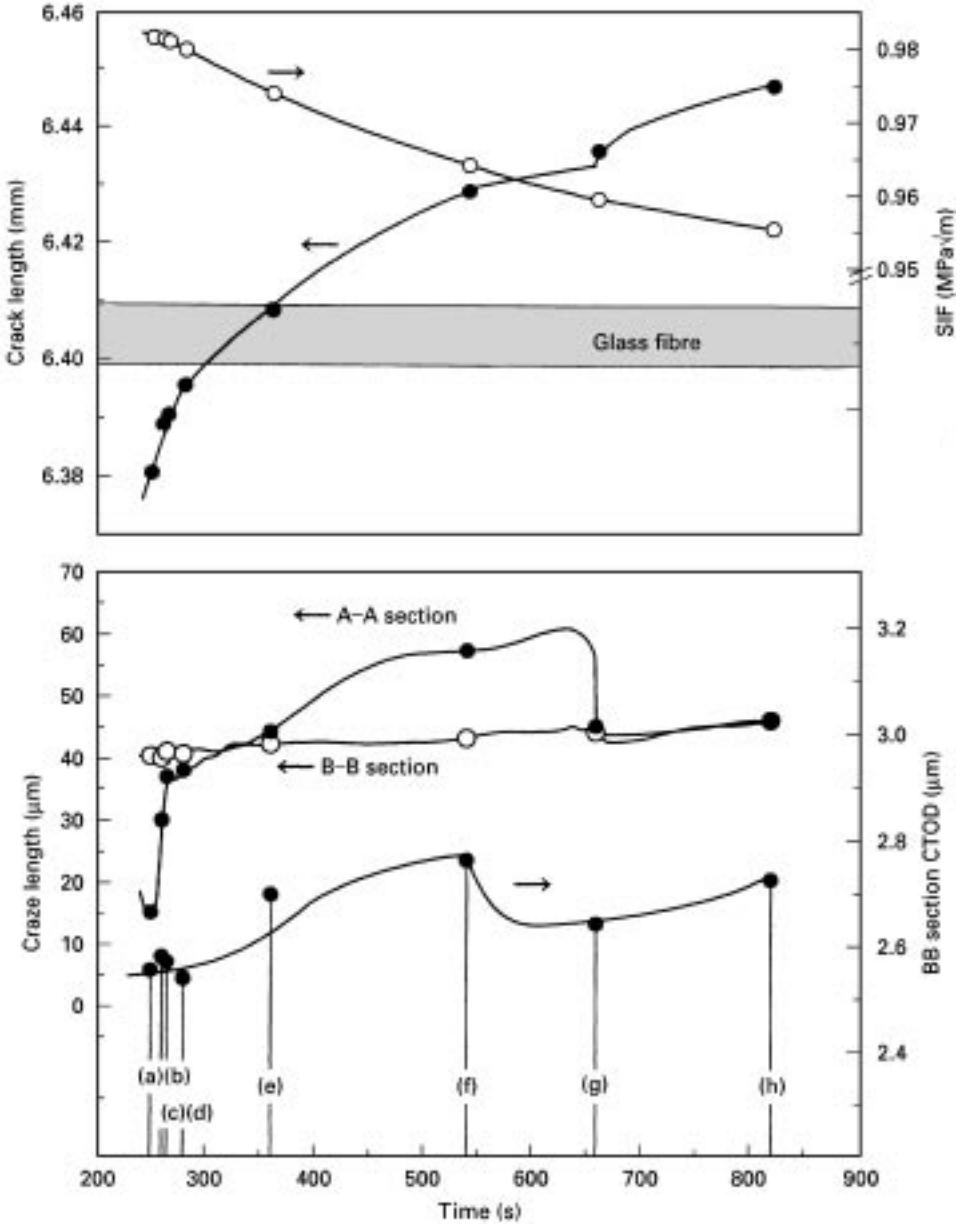

Figure 5 Variation of (a) (●) crack length (○) stress intensity factor – (SIF), and (b) craze length along sections (●) A–A and (○) B–B and (▲) crack tip opening displacement (CTOD) during crack growth shown in Fig. 4. The sections A–A and B–B are defined in Fig. 4a.

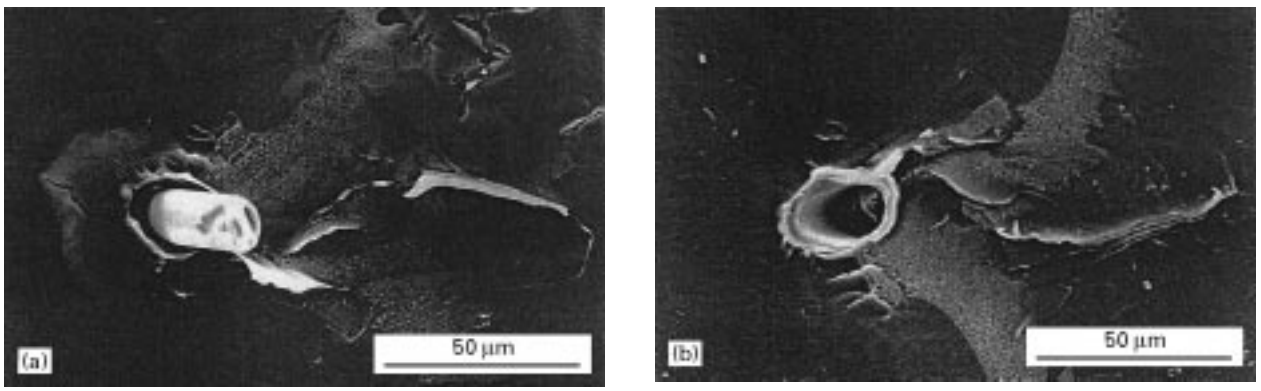

Figure 6 Upper and lower fracture surfaces associated with the arrest line around the glass fibre during crack growth of Fig. 4.

opening along the line A–A crossing the fibre, and the dashed curves are that along the line B–B far away from the fibre. The crack opening is suppressed over a region about 30 μm away from the craze tip side the right side of the fibre. This distance seems to be independent of the position of the fibre. However, the crack trajectory at the crack side (the left side) is not so affected by the presence of the fibre. At stage (h), where the fibre is inside the crack, the crack trajectory at section A–A becomes nearly equal to that to section

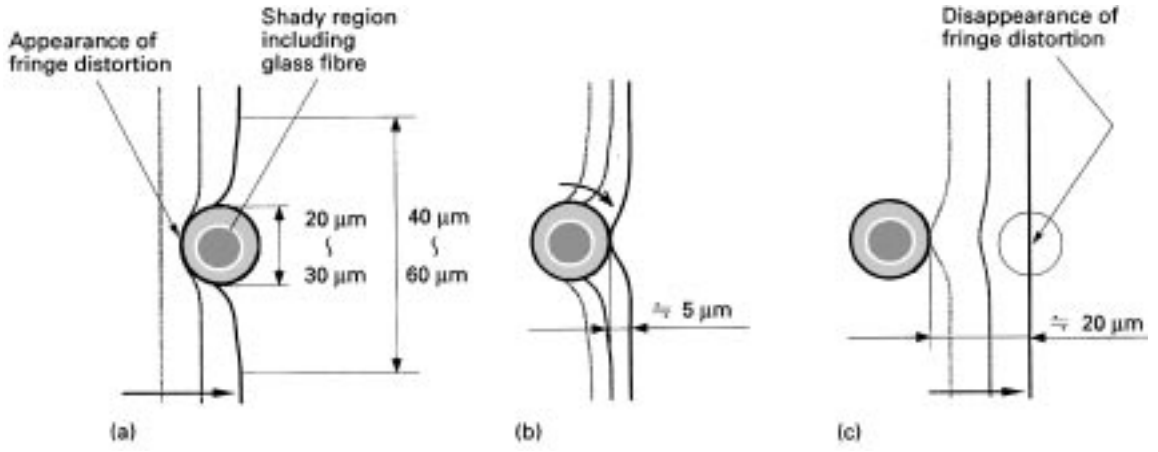

Figure 7 Schematic illustration of the distortion of fringe marks around a glass fibre observed when a crack (a) encounters the fibre, (b) crosses the fibre (b) and (c) departs from the fibre. The lengths marked, indicate of the extent of distortion of the fringe marks.

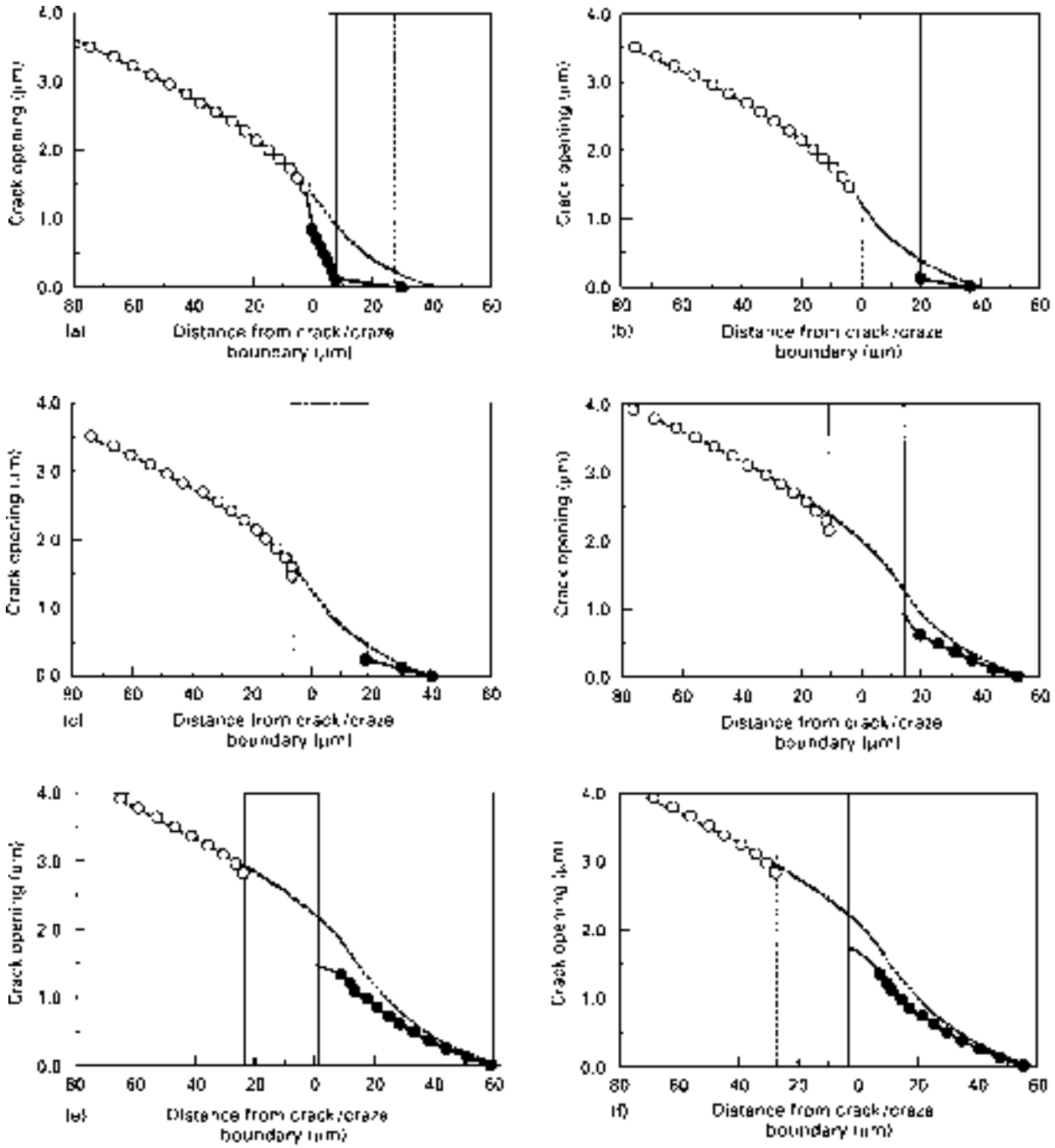

Figure 8 Variation of crack opening along (—) A–A and (– – –) B–B during crack growth shown in Fig. 4. Sections A–A and B–B are defined in Fig. 4. The glass fibre is included in the shaded parts. Deformation (●) in and (○) out of the craze zone, are shown.

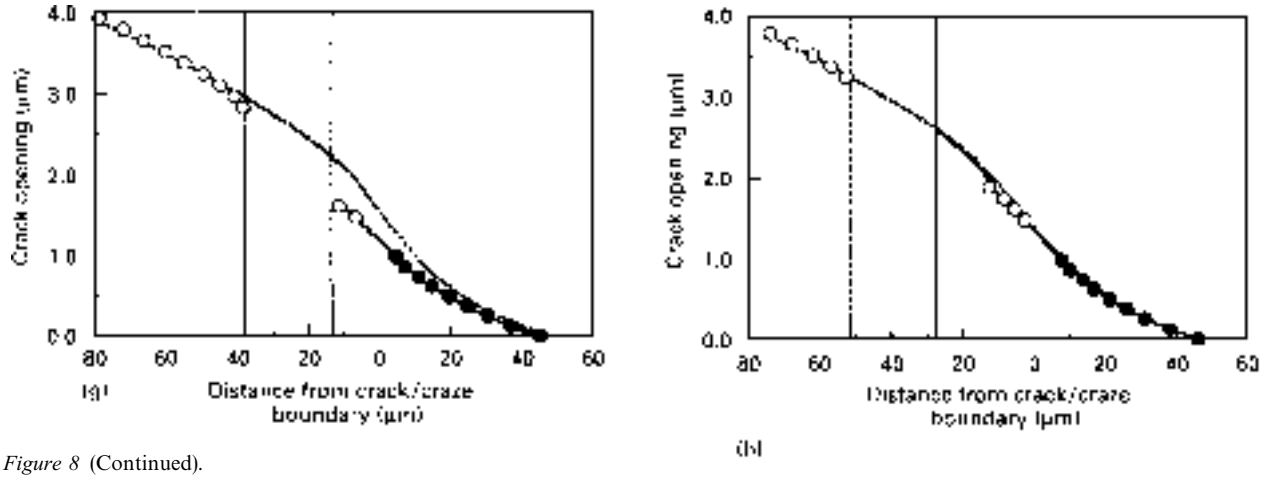

Figure 8 (Continued).

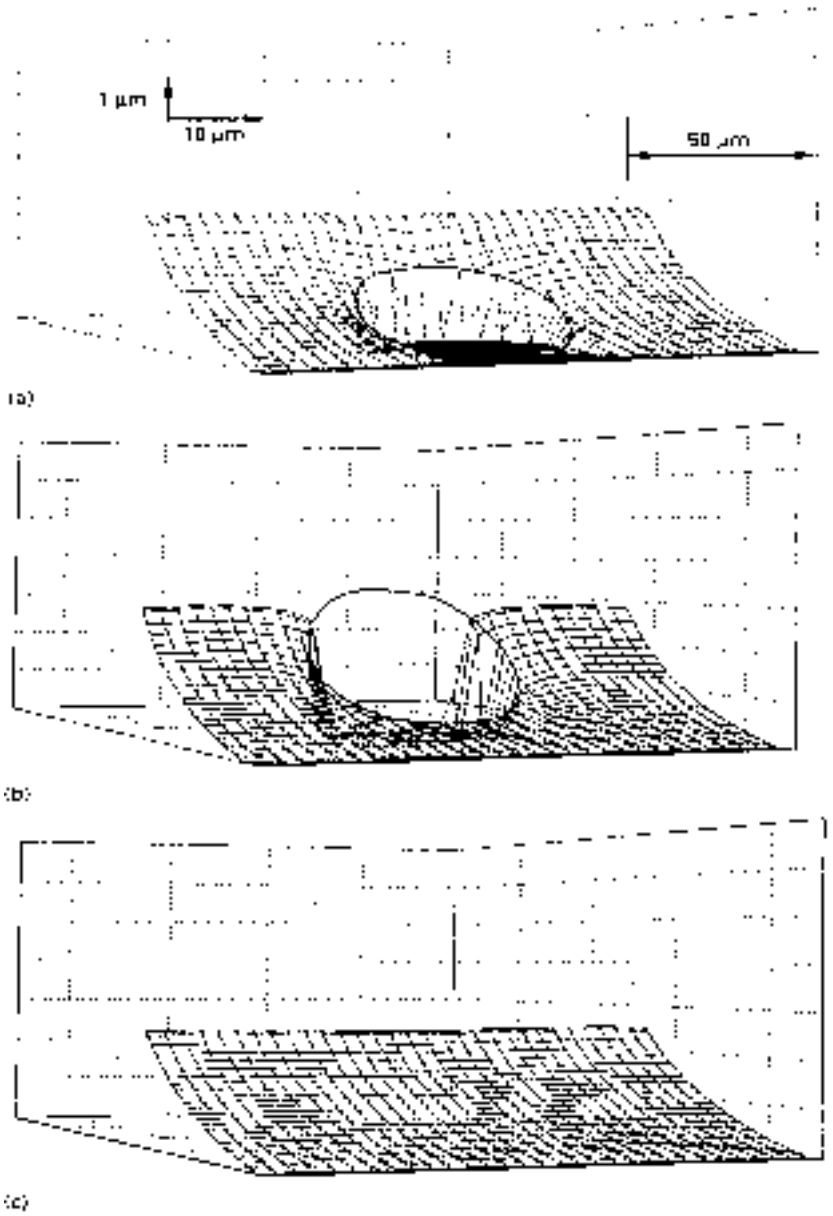

Figure 9 Three-dimensional expressions of craze opening around a glass fibre. (a) (b) and (c) correspond to (a), (d) and (h) in Fig. 4, respectively.

B–B, while the fringe marks are still distorted slightly. At this stage, the fibre probably breaks and the crack begins to grow again in a rapid manner, leaving the arrest line shown in Fig. 6.

Fig. 9 represents the three dimensional expressions corresponding to stages (a), (d) and (h) in Fig. 4. These are numerically drawn, based on the fringe patterns observed. From these, the

bridging effect due to the fibre may be understood visually.

Another example of the fringe pattern distortion when the crack crosses the fibre is shown in Fig. 10. The same conclusions as for at the example mentioned above, may be derived.

For the fringe pattern distortion during crack growth is shown in Fig. 11, where the fracture surfaces are also indicated. When the crack grows just above the fibre parallel to the crack growth direction (a) the distorted region of the fringes is relatively large, but the degree of distortion is small. Cavities formed during the injection-moulding process (b) and the tear lines developed along the crack direction (c), distort the fringe patterns. However, these small defects do not seem to leave arrest lines on the fracture surfaces. They may not offer a strong resistance to the crack growth. Generally, the fibres which are poorly bonded to the matrix or are parallel to the fracture surface do not produce distortion of the fringe mark very much.

The fracture surfaces of samples including SGF, contents of 0, 0.1 and 0.2 wt % are shown in Fig. 12. The number of arrest lines increases with increasing SGF fraction. The arrest lines for the specimen without SGF were made intentionally by dropping the applied load. In addition to these arrest lines, glass fibers or small cavities always exist adjacent to the arrest lines. The load required for crack growth increases with increasing SGF weight fraction. It is clearly understood from the above discussion that the glass fibre offers a high resistance to crack growth.

4. Conclusion

In order to investigate the effect of glass fibre on the crack growth in FRP, the crack opening behaviour

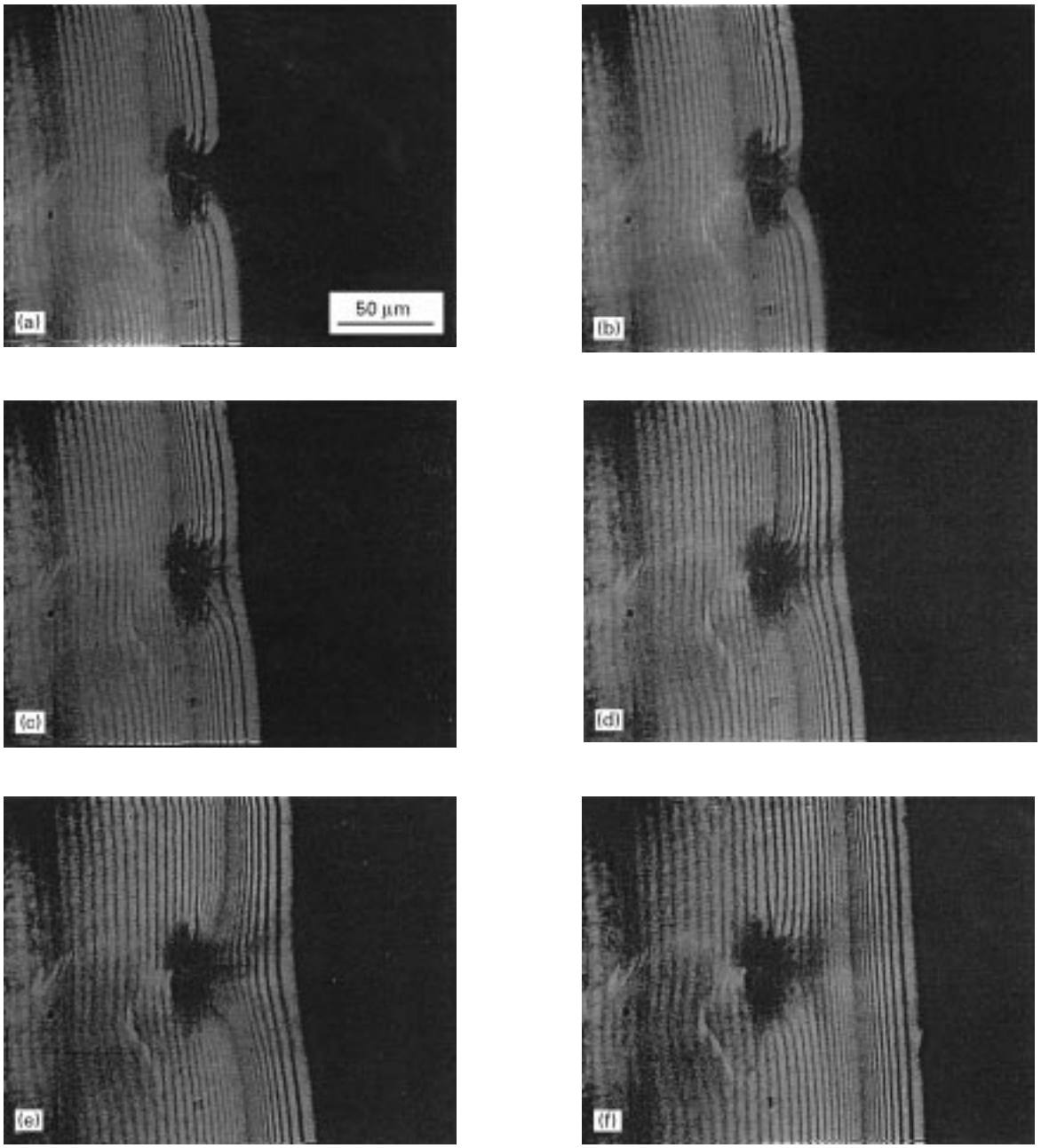

Figure 10 Another example of the variation of fringe patterns during crack growth around a glass fibre perpendicular to the crack planes.

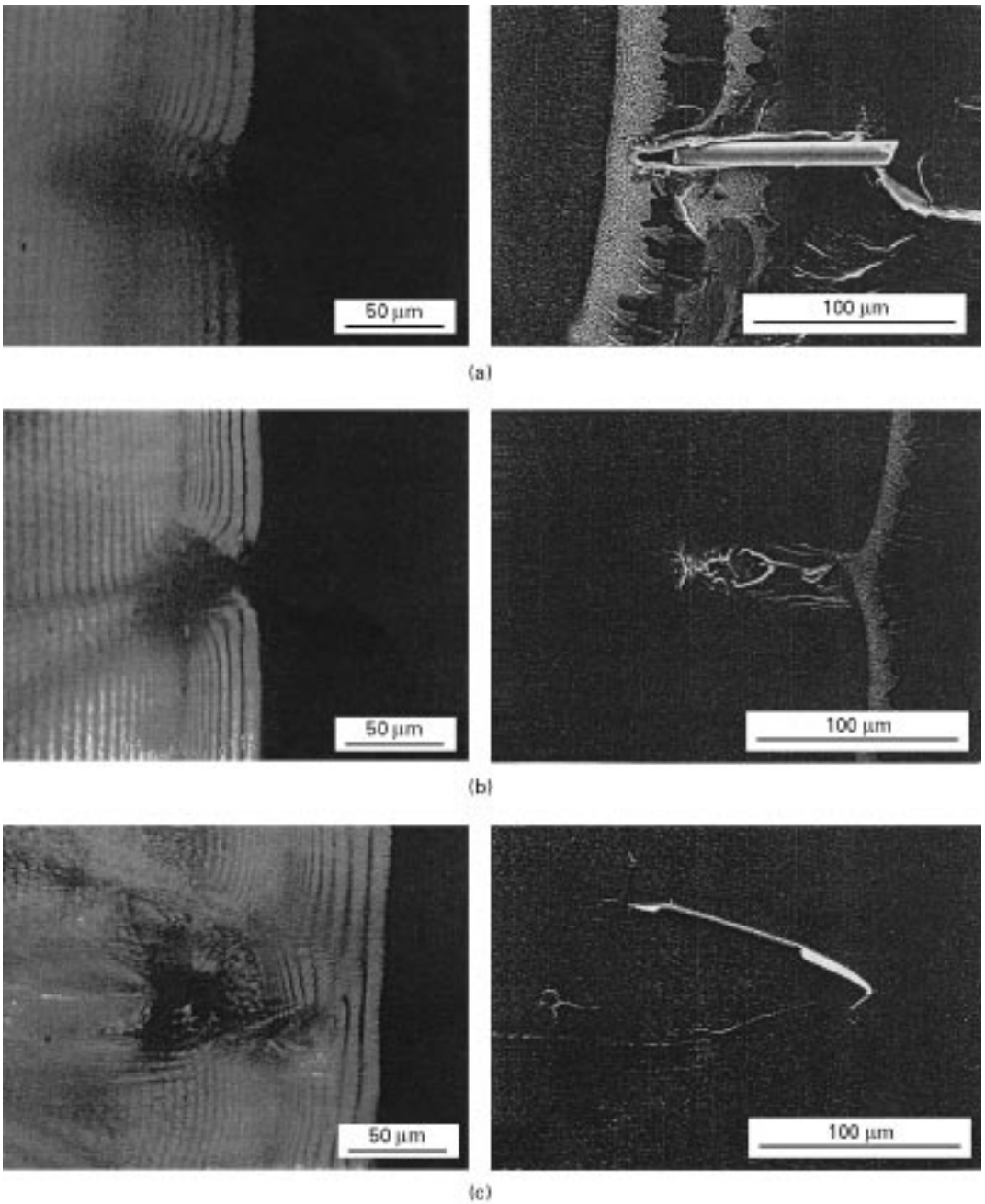

Figure 11 Examples of fringe patterns distorted by (a) glass fibres parallel to the crack planes, (b) a cavity included during injection moulding, and (c) tear lines made by crack growth and their corresponding fracture surfaces.

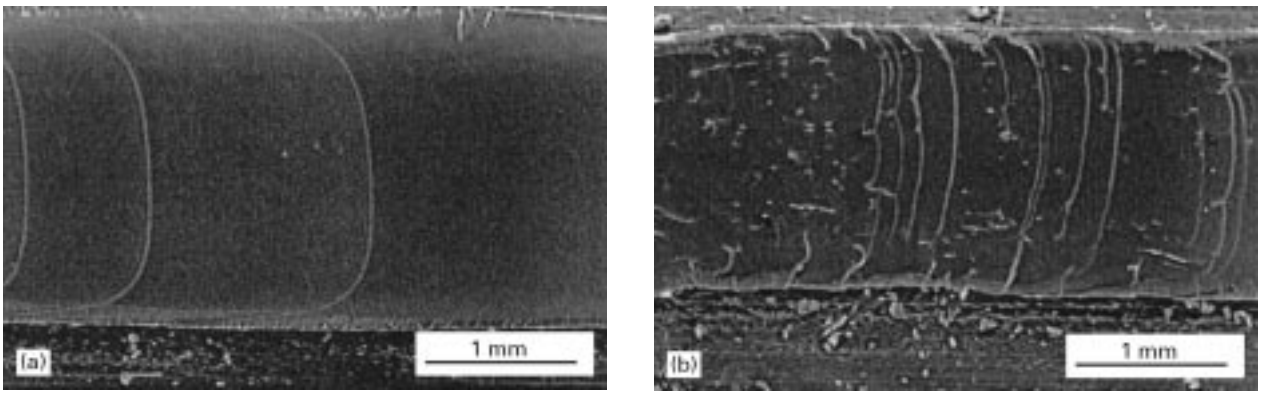

Figure 12 Fracture surfaces associated with arrest lines for different fractions of glass fibre (a) 0 wt % (b) 0.1 wt % and (c) 0.2 wt %.

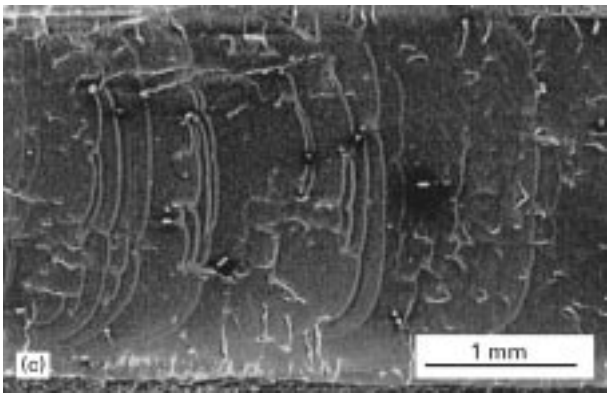

Figure 12 (Continued).

when the crack crosses the fibre was observed by optical interferometry. Optical interferometry is a very powerful tool for investigating crack/fibre interaction, because the crack deformation behaviour can be visually observed in real time. However, the probability of a clean fringe pattern being recorded through a microscope is very low. For samples with a relatively high content of glass fibres for example 0.2 wt %, it is difficult to obtain any clean fringe pattern because many arrest lines and tear lines remain on the crack planes. The specimens with SGF contents much smaller than 0.1 wt % may be useful for obtaining clear fringe marks.

In this work, it was shown that when the crack crosses the fibre, the fibre distorts the fringe pattern, decreasing the crack growth velocity and leaving arrest lines around it, therefore, the fibre after a great resistance to crack growth.

Acknowledgements

The authors thank Mr K. Ishii, student of our university, for his technical assistance.

References

1. K. FRIEDRICH, in a "Fractography and Failure Mechanics of Polymers and Composites", edited by A. C. Roulin-Moloney, (Elsevier Applied Science, New York, 1989) p. 437.
2. W. DÖLL, in "Crazing in Polymers, Advances in Polymer Science 52/53", edited by H. H. Kaush (Springer, Berlin, 1983) p. 105.
3. W. DOLL and L. KONCZOL in "Crazing in Polymers", Vol. 1.2," Advances in Polymer Science 91/92", edited by H. H. Kaush, (Springer, Berlin, 1990) p. 137.
4. R. SCHIRRER, *ibid*., p. 215.
5. M. KITAGAWA, N. KOYAMA, T. CHIKAMATSU and M. TAKEMORI, *Soc. Mater. Sci. Jpn* **43** (1994) 1094.
6. N. KOYAMA, M. KITAGAWA and M. TAKEMORI, *Trans. Jpn Soc. Mech. Eng. A* **61** (1995) 1480.
7. D. S. Dugdale, *J. Mech. Phys. Solids* **8** (1960) 100.
8. J. R. RICE, in "Fracture- an advanced treatise" edited by H. Liebowitz Academic Press New York, 1968) p. 191.

Received 5 November 1997
and accepted 22 April 1998